ELSEVIER

International Journal of Mass Spectrometry 216 (2002) 115–128

International Journal of Mass Spectrometry

www.elsevier.com/locate/ijms

Classical theories of the ion/linear quadrupole capture

Jan Turulski[a], Timothy Su[b,*], Jan Niedzielski[c], Barbara Pezler[d]

[a] *Chemistry Institute, University of Bialystok, 15-370 Bialystok, Poland*
[b] *Department of Chemistry and Biochemistry, University of Massachusetts Dartmouth, Dartmouth, MA 02747, USA*
[c] *Chemistry Department, Warsaw University, 02-089 Warsaw, Poland*
[d] *Chemistry Department, Agricultural and Teacher's University, 08-110, Siedlce, Poland*

Received 27 September 2001; accepted 31 January 2002

This paper is devoted to the memory of Professor Walter Chesnavich whose pioneering contribution
to the theory of ion/molecule reactions cannot be underestimated.

Abstract

The dependence of the ion/linear quadrupole capture rate constant on the resultant orbital-rotational momentum and individual energetic and molecular parameters that characterize a given system are calculated using a microcanonical version of the transition state theory and classical trajectory method. Both methods indicate that the dependencies are similar to those obtained for the ion/linear dipole system. It is shown that, contrary to the ion/polar molecule systems, the capture rate constant for the quadrupoles frequently does not fall on the plateau which corresponds to the assumption that the resultant momentum can be approximated to the orbital momentum. Therefore, the theories that use this approximation are not adequate for description of the ion/quadrupole capture. Both TST and classical trajectory calculations agree very well with experiment and give identical or slightly different results for $|b_3| \leq 10$ which covers the whole range of temperatures down to extremely low. At so low temperatures the discrepancies are larger which seems to be of little consequence since both methods do not account for the quantum effects. (Int J Mass Spectrom 216 (2002) 115–128) © 2002 Elsevier Science B.V. All rights reserved.

---

1. Introduction

Generally, the nonspherically symmetrical potential describes interactions between ions and molecules. When it comes to collision, apart from the total energy *E*, that is the sum of translational and rotational contributions, the resultant total angular momentum *J*, that includes contributions from the orbital angular momentum *l*, and the rotational momentum *j*, has to be conserved. The dependence of the classical Hamiltonian on *J* is very intricate. For this reason a simplified dependence on *l* and *j* is most frequently used [1–12].

$$H = \frac{p_r^2}{2M_r} + \frac{l^2}{2I_1} + \frac{j^2}{2I_2} + V(r,\gamma) \equiv \frac{p_r^2}{2M_r} + H^* \quad (1)$$

where $I_1 = M_r r^2$, $I_2 \equiv I$ is the moment of inertia of the linear quadrupole, M_r is the reduced mass of the system, r is the distance between the point ion and the centre of mass of the quadrupole, and γ is the angle the quadrupole axis makes with r. $V(r,\gamma)$ in Eq. (1) is the interaction potential. Ignoring the anisotropy of the quadrupole polarizability we can express this potential as:

$$V(r,\gamma) = -\frac{\alpha q^2}{2r^4} + \frac{Qq}{2r^3}(3\cos^2\gamma - 1) \quad (2)$$

---

[*] Corresponding author. E-mail: tsu@umassd.edu

1387-3806/02/$ – see front matter © 2002 Elsevier Science B.V. All rights reserved.
PII S1387-3806(02)00559-6

where α is the polarizability and Q the static quadrupole moment of the quadrupole and q is the electrical charge on the ion.

Hamiltonian (1) combined with the law of total angular momentum conservation defines the capture rate. The conservation of total angular momentum can be expressed as:

$$\delta(\boldsymbol{J} - (\boldsymbol{I} + \boldsymbol{j})) = h(J - |l - j|)h(l + j - J) \qquad (3)$$

where J is the length of the $\boldsymbol{J}$ vector, l is the length of the $\boldsymbol{I}$ vector, j is the length of the $\boldsymbol{j}$ vector, and $\delta(x)$ and $h(x)$ denote the delta functions of Dirac and Heaviside, respectively. There are different theoretical methods to estimate the capture rate constant in the ion/molecule system. The microcanonical version of the transition state theory (TST) is likely the simplest [10]; k_1 is assumed to correspond to the minimum rate at which the flux of reagents crosses the surface S^* separating the substrates and products in the phase space. Assuming the spherical form of $S^* : \{r = r^* \equiv \text{const.}\}$ we obtain:

$$k_1(E, J) = \min_{r^*} k_1(E, J; r^*) = \frac{1}{2\pi\hbar} \min_{r^*} \frac{\int h(E - H^*)\delta(J - (l + j))\,\mathrm{d}\Gamma^*}{\rho_0(E)} \qquad (4)$$

where $\rho_0(E) = I(2M_{\mathrm{r}}E)^{3/2}/3\pi^2h^5$ and

$$\mathrm{d}\Gamma^* = \frac{\sin\gamma\,\mathrm{d}l\,\mathrm{d}j\,\mathrm{d}\gamma}{2\hbar^2} \qquad (5)$$

While the capture rate constant k_1, for the ion/polar molecule system is very well characterized using different theoretical approaches [1–11], complete calculations for the ion/quadrupole system were only performed by Troe and coworkers with use of the classical trajectory method (CT) [12].

One of the versions of the latter method has been developed by Su et al. [3–5,14,17,24]. We use this version in this work. The CT capture rate constant is estimated from

$$k_1 = \frac{1}{2IkT(2\pi M_{\mathrm{r}}kT)^{1.5}} \times \int \chi_r\{p, q\} \cdot e^{-E/kT} \mathrm{d}\gamma_l\,\mathrm{d}\gamma_j\,\mathrm{d}l\,\mathrm{d}j\,2J\,\mathrm{d}J\,\mathrm{d}E \qquad (6)$$

where γ_l and γ_j are Euler angles, $\chi_r\{p, q\}$ is the characteristic function which labels the trajectory with initial conditions $\{p, q\}$ on r as reactive or nonreactive. Trajectories are integrated from 50 Å toward the capture radius. The method used in the present calculation is similar to that described previously [24] except that 20,000 trajectories are used for each system.

Estimations of k_1 for the ion/polar molecule system indicate that, irrespective of the calculational method used, the classical capture rate constant is a function of two dimensionless parameters. There is some arbitrariness in the choice of these parameters. Some authors opt for such a pair whose one component depends on the molecular parameters exclusively, while another one also depends on the energy/temperature [10,14]. Another approach has been developed in which both parameters depend on the energy/temperature. According to the first parametrization, the ion/dipole capture rate constant increases as the energy/temperature decreases, as is evidenced by the changes in the energetical parameter. For a given energy/temperature the second, purely molecular, dimensionless parameter describes the system in a very characteristic way. At exceptionally small values of this parameter, k_1 is also small, and relatively insensitive to the changes in this parameter. It is the region of the first plateau. Once a certain threshold value has been surpassed, k_1 starts to exhibit a nearly linear increase with increasing value of the molecular parameter to reach another plateau, termed by us as the Su-Chesnavich plateau, at some limiting value [10]. The capture rate constant is much larger over this second plateau than over the first one. It was shown, using the TST approach [15], that over the first plateau the molecules are so highly excited that the assumption $J \cong j$ holds. Conversely, over the second plateau we can assume that $J \cong l$. A comparison with experiment indicates that practically all of the ion/dipole reactions are well described using the second assumption. There is inconclusive evidence [16] that some scarce reactions occur over the transitional region between the first and second plateau.

The ion/quadrupole systems have been studied less extensively. Nevertheless, k_1 has also been found to depend on two dimensionless parameters, similar but not identical with those used for the ion/dipole systems. Bhowmik and Su [17] estimated the k_1 dependence on the moment of inertia for the model reaction $D_3^+ + C_6F_6$. The form of this dependence was the same as the k_1 dependence on the dimensionless molecular parameter. It is worth noting that for this particular system the dependence is qualitatively the same as that observed for the ion/dipole systems: the first plateau, then an increase with increasing molecular parameter, finally the second plateau. The work performed by Troe and coworkers was more general [12]. Unfortunately, these authors chose another version of parametrization, both dimensionless parameters depending on the energy/temperature. Thus, a direct comparison with the results of Bhowmik and Su is difficult. Bearing in mind the simplicity of the TST method it seems worthwhile to investigate the k_1 dependence on both parameters to make comparison with the CT results as well as experimental measurements.

2. TST calculations and comparison with the CT method

Substituting $r = (\alpha q^2/2E)^{0.25}R$ into Hamiltonian (1) we obtain:

$$H^* = E\left[\frac{l^2}{a} + j^2 - \frac{1}{R^4} + \frac{B_3}{R^3}(3\cos^2\gamma - 1)\right] \qquad (7)$$

where $a = (B_3)^2\zeta R^2$. The definition of variables is altered: $j \rightarrow (2I_1E)^{0.5}j$ and $l \rightarrow (2I_2E)^{0.5}l$. The element of the phase space volume $\mathrm{d}\Gamma^*$ can now be given as:

$$\mathrm{d}\Gamma^* = E(I_1I_2)^{1/2}\frac{\sin\gamma\,\mathrm{d}l\,\mathrm{d}j\,\mathrm{d}\gamma}{2\hbar^2} \qquad (8)$$

It is seen that the Hamiltonian for the ion/linear quadrupole system depends on the two coefficients, B_3 and ζ which are defined as:

$$B_3 = \frac{Qq}{(2E\alpha^3q^6)^{1/4}} \qquad (9)$$

$$\zeta = \frac{M_\mathrm{r}\alpha^2q^2}{IQ^2} \qquad (10)$$

Substituting $E \rightarrow kT$ into Eq. (9) we obtain the b_3 coefficient, which is a temperature analog for B_3.

Such a type of parametrization seems to be the simplest used in the theories of ion/quadrupole capture. Instead of B_3 or b_3 some authors choose to adopt their equivalents or for instance, they use $I^* = \zeta^{-1}$ instead of ζ. These differences are only a matter of taste and convenience. Substituting Hamiltonian from Eq. (7) into Eq. (4) we obtain after simple transformations:

$$\kappa_1 \equiv \frac{k_1(E,J)}{k_L} = \min_{R=R^*}[\kappa_1(E,J;R)] \qquad (11)$$

where $k_L = 2\pi q(\alpha/M_\mathrm{r})^{0.5}$ and

$$\kappa_1(E,J;R) = \frac{3}{4(B_3)^2\zeta}\iiint h(\varepsilon_0 - \varepsilon_z z^2)\frac{z}{2}\,\mathrm{d}z \times h(J - |l - j|)h(l + j - J)\,\mathrm{d}l\,\mathrm{d}j \qquad (12)$$

where

$$\varepsilon_0 = 1 + \frac{1}{R^4} - \frac{l^2}{a} - j^2 + \frac{B_3}{R^3} \qquad (13)$$

$$\varepsilon_z = \frac{3B_3}{R^3} \qquad (14)$$

$$z = \cos\gamma \qquad (15)$$

$$\varepsilon_\mathrm{min} = \left(\text{if } B_3 > 0 \text{ then } \left(1 + \frac{1}{R^4} - \frac{2B_3}{R^3}\right) \times \text{else } \left(1 + \frac{1}{R^4} + \frac{B_3}{R^3}\right)\right) \qquad (16)$$

Integration over the variable from Eq. (12) gives:

$$\kappa_1(E,J;R) = \frac{3}{4(B_3)^2\zeta}\begin{cases} \iint h(\varepsilon_0 - \varepsilon_z)h(J - |l - j|)h(l + j - J)\,\mathrm{d}l\,\mathrm{d}j & \text{for } \varepsilon_\mathrm{min} > 0 \\ \iint \sqrt{\dfrac{\varepsilon_0}{|\varepsilon_z|}}h(\varepsilon_0)h(-\varepsilon_0 + \varepsilon_z)h(J - |l - j|)h(l + j - J)\,\mathrm{d}l\mathrm{d}j & \text{for } \varepsilon_\mathrm{min} < 0 \end{cases} \qquad (17)$$

Further integration over l and j is cumbersome and only partially can be solved analytically. It will not be given here. The final result of partially numerical integration is the dependence of the function κ_1 (E, J; R) defined in Eq. (12) on the variable R. The numerical minimization of this function over R gives the reduced microcanonical capture rate constant κ_1 (E, J) which depends on energy through B_3. The examples given in Fig. 1 show the relation of TST κ_1 against J (through the reduced momentum $= J/(2IE)^{0.5}$) for some systems that differ in the values for ζ. The first model system (Fig. 1A) features a negative Qq, so that $B_3 = -5$ whilst the second one (Fig. 1B) features a positive Qq, so that $B_3 = +5$. For the other values of B_3, the relations are similar; only the range $0 \le J \le J_{\max}$ is increasing as B_3 increases. In other words, $J_{\max}$ increases as does B_3. If ζ is small so is this enhancement; for such systems $J_{\max}$ is close to unity. However, at larger ζ an increase in B_3 is accompanied by the marked increase in $J_{\max}$. Numerical integration of TST κ_1 (E, J) over momentum leads to the microcanonical TST capture rate constant κ_1 (E)

$$\kappa_1(E) = \int_0^{J_{\max}} \kappa_1(E, J) 2J\,\mathrm{d}J \qquad (18)$$

For obvious reasons κ_1 (E) depends only on B_3 and ζ. A form of such dependence is shown in Fig. 2. Fig. 2A and B show κ_1 vs. $\log\zeta$ for the systems that feature $B_3 < 0$ and $B_3 > 0$, respectively. The qualitative resemblance to the corresponding dependencies obtained for the ion/dipole systems [10] is striking. At vanishingly small values for ζ, κ_1 is practically constant. Only after the critical value for ζ has been exceeded is an enhancement in κ_1 observed. This critical value is the larger the smaller the B_3, hence the larger the energy of the system. At some value of ζ a distinct maximum is visible, the magnitude of which being always larger for the negative than the positive B_3. Compared with the corresponding ion/dipole systems, the maximum is smaller. Further increase in ζ results in a decrease in κ_1 down to the plateau value. The capture rate constant over this Su-Chesnavich plateau is much larger than over the first plateau, as in the case of the ion/dipole systems [10]. It can be concluded that high rotational excitation of a molecule decreases the capture rate.

Thermodynamic averaging of TST κ_1 (E) using the weight corresponding to five d.f. (three translational and two rotational) yields the temperature dependence through b_3. As can be seen from Eq. (6) a canonical formalism used in the CT method gives the capture rate constant in the form already averaged.

A comparison with experiment is now possible. Fig. 3 shows examples of the κ_1: dependence on $\log\zeta$ for a few selected values of b_3. Both TST and CT κ_1 are shown. The relations are similar to those obtained before averaging except for the fact that κ_1 is diminished and the maximum separating the regions of the first and the second plateau is nearly extinct.

Inspection of Fig. 3 indicates that both CT and TST give $\kappa_1(\log\zeta)$ qualitatively similar for all b_3. At $|b_3|$ not too large, say $|b_3| < 10$, the differences never surpass 5%. However, at larger $|b_3|$ the differences can be as large as even 10%. Even though according to the kinetic variational principle $k^{\mathrm{TST}} \ge k^{\mathrm{CT}}$ so large a difference seems to result from inaccuracies of calculations. Any efforts to make more sophisticated calculations would not make much sense because at extremely low temperatures (large $|b_3|$) classical approaches are obviously inadequate.

Note that so far κ_1 vs. ζ was investigated indirectly and for a single model system. Bhowmik and Su [17] used the CT method to investigate the capture of C_6F_6 by D_3^+ at 300 K. For extremely small moment of inertia, which corresponds to large ζ, they found that κ_1 is also large, 1.49. For the corresponding $b_3 \cong 3$ our estimate is 1.50. The agreement is excellent, at least over the Su-Chesnavich plateau. The agreement is also most satisfactory for large I (equivalent to very small ζ). However, the real value for I for the C_6F_6 quadrupole is 692.26 amu A^2 [17] which corresponds to $\zeta = 0.06$. Inspection of Fig. 3B as well as Fig. 1 in [17] reveals that the capture rate constant falls on the transitional region between the plateaus. So do the capture rate constants for many reactions that feature rather small values for ζ (see Tables 4–6). At ζ sufficiently large, in the absence of any restrictions such as selection rules etc., the capture rate constant does not

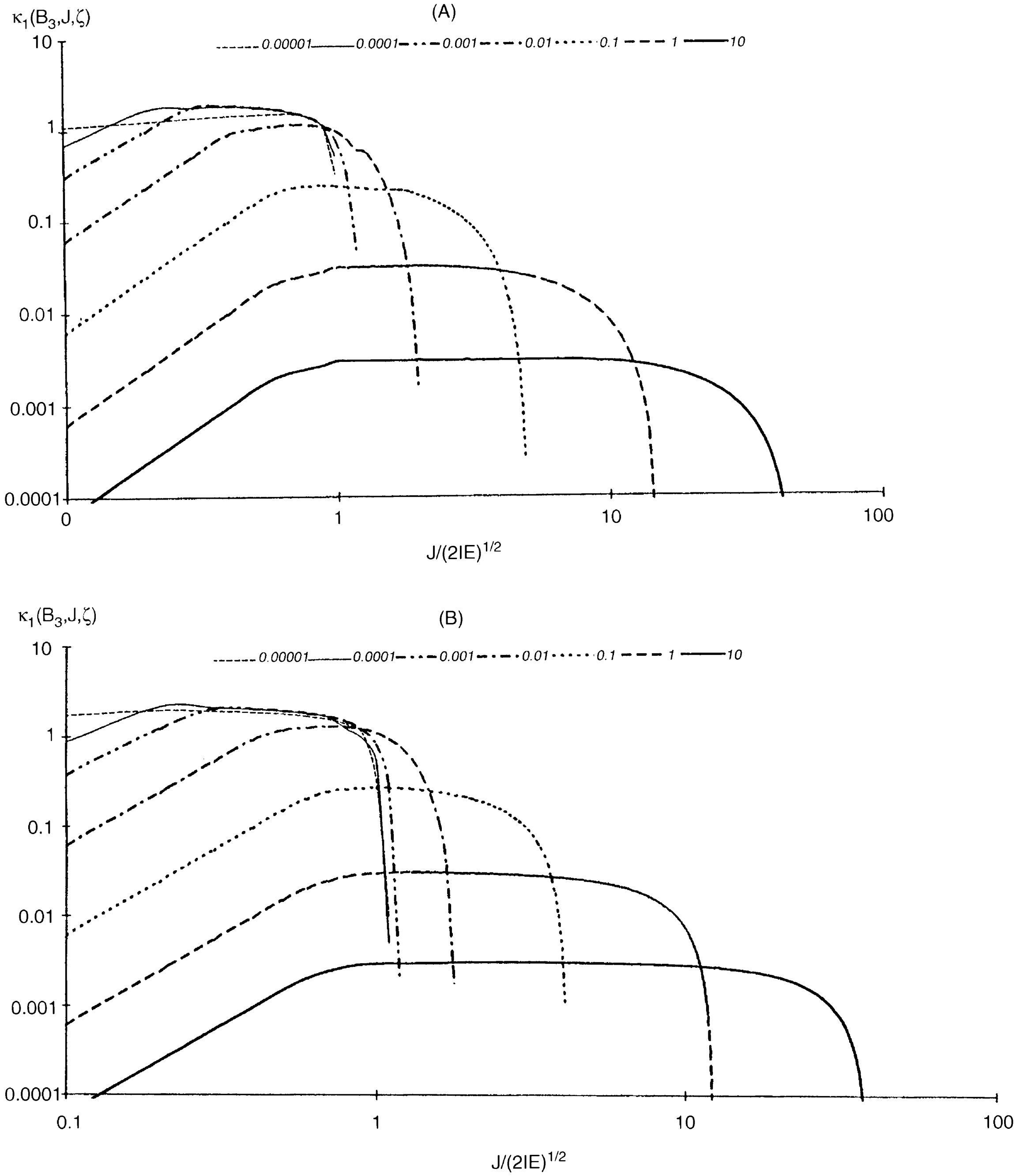

Fig. 1. Examples of the dependence of the reduced microcanonical capture rate constant on the resultant momentum J expressed in $(2IE)^{1/2}$ units. (A) $B_3 = -5$, (B) $B_3 = +5$; the curves are labeled with different values for ζ.

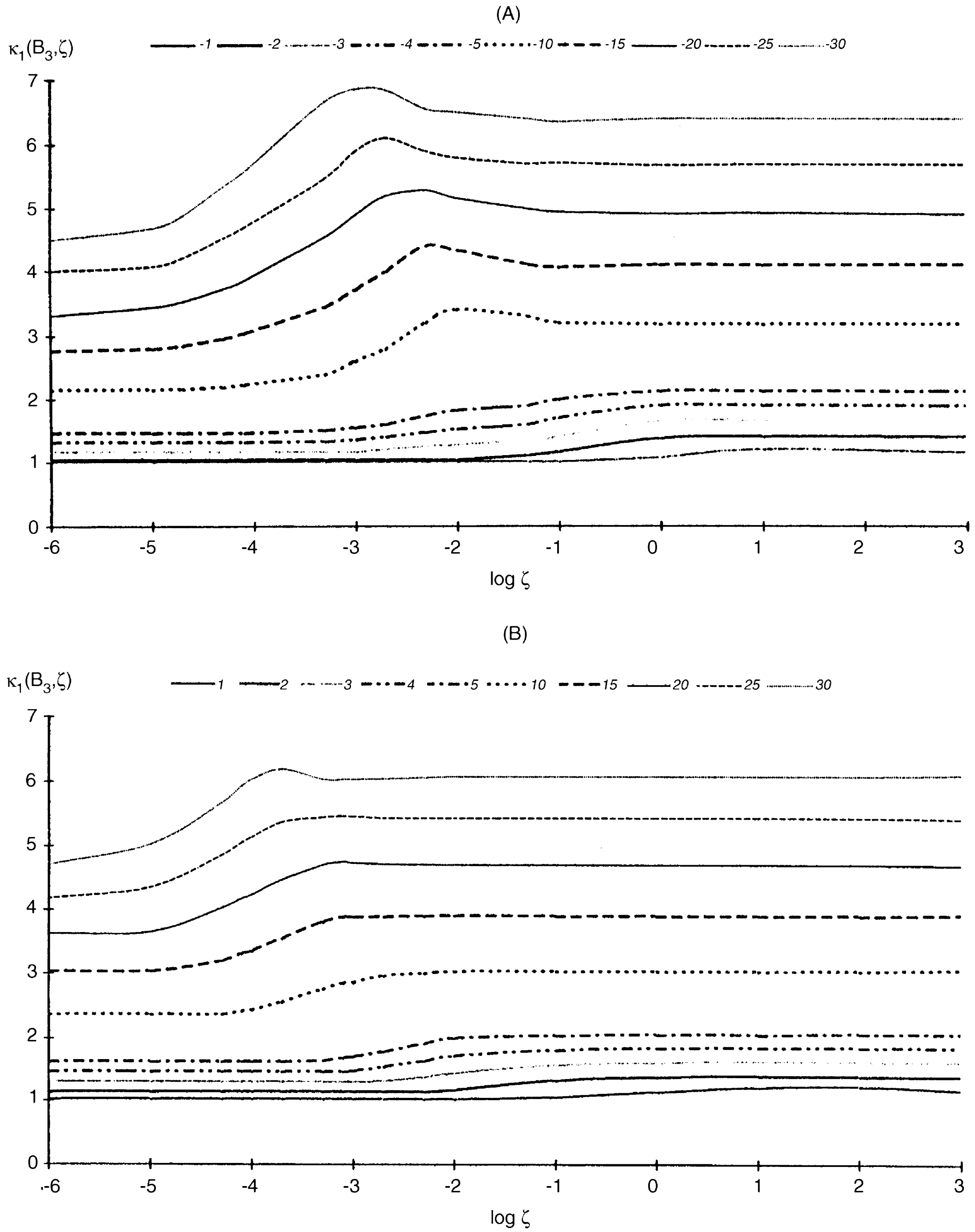

Fig. 2. Examples of the dependence of the reduced microcanonical capture rate constant on $\log \zeta$. The curves are labeled with different values for B_3. (A) Odd case, (B) even case.

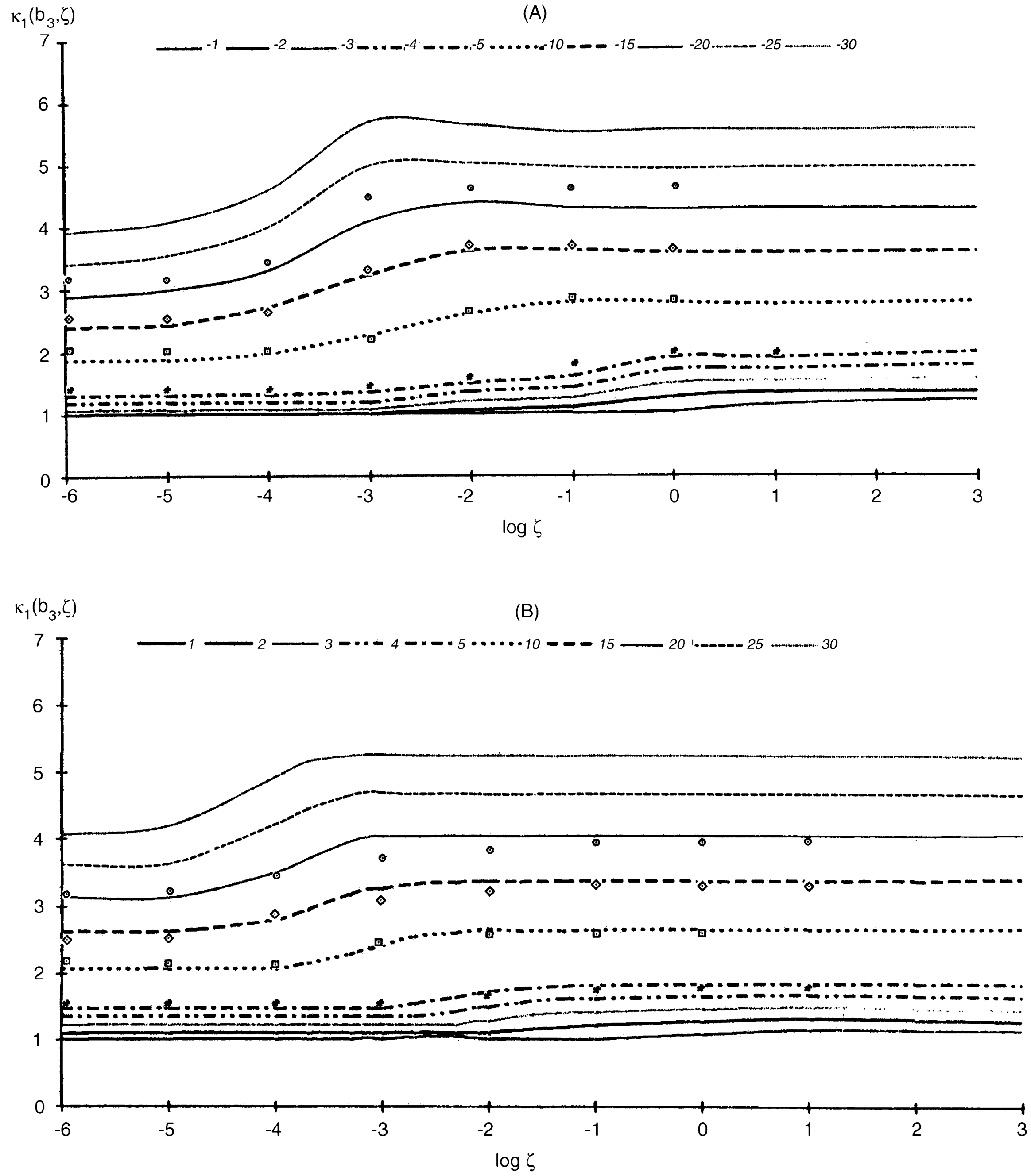

Fig. 3. Examples of the dependence of the thermodynamically averaged reduced capture rate constant on $\log \zeta$. Symbols alongside the curves correspond to κ_1^{CT}; stars—$|b_3| = 5$; squares—$|b_3| = 10$; diamonds—$|b_3| = 15$; circles—$|b_3| = 20$. The curves that represent the TST estimates are labeled with different values for b_3. (A) odd case, (B) even case.

show any dependence on ζ. If any restrictions are imposed, κ_1 vs. ζ exhibits erratic behavior. Obviously ζ is not a decisive factor. At very small ζ, in the absence of any restrictions, κ_1 should increase slightly as ζ increases. A condition of b_3 conservation requires that the temperature be constant, and the same molecule be involved. Thus, any change in ζ can only result from the changes in ion identity. To be strict, only the ion mass is important since ζ is proportional to the reduced mass of the system. It can be concluded that in simple ion/quadrupole captures κ_1 increases slightly with increasing mass of the ion, as is indeed confirmed by the data shown in Tables 5 and 6. It is not in accord with Mendas and Milutinovic [21] who examined a series of reactions $C_6F_6 + X^+$ and c-$C_6H_{12} + X^+$ and found no dependence of κ_1 on ζ. Apparently, these authors considered reactions occurring at different temperatures, and, hence, apart from ζ also b_3 contributed to the final result.

Since ζ is inversely proportional to the quadrupole moment squared while in ion/polar molecule captures the proportionality to the inverse dipole moment is obeyed, ion/quadrupole captures that occur over the transitional region between the first and second plateau are fairly numerous in contrast to the ion/polar molecule captures. Unfortunately, while κ_1 over the plateau can easily be obtained in the nearly analytical form [15], over the transitional region we have to resort to onerous numerical calculations. An attempt can be made to fit an empirical relation to the obtained relations but it does not much alleviate the problem. Fig. 4 shows a few examples of κ_1 (b_3) for a number of selected ζ. The data from both the plateau regions are included [15]. Using the least squares method we

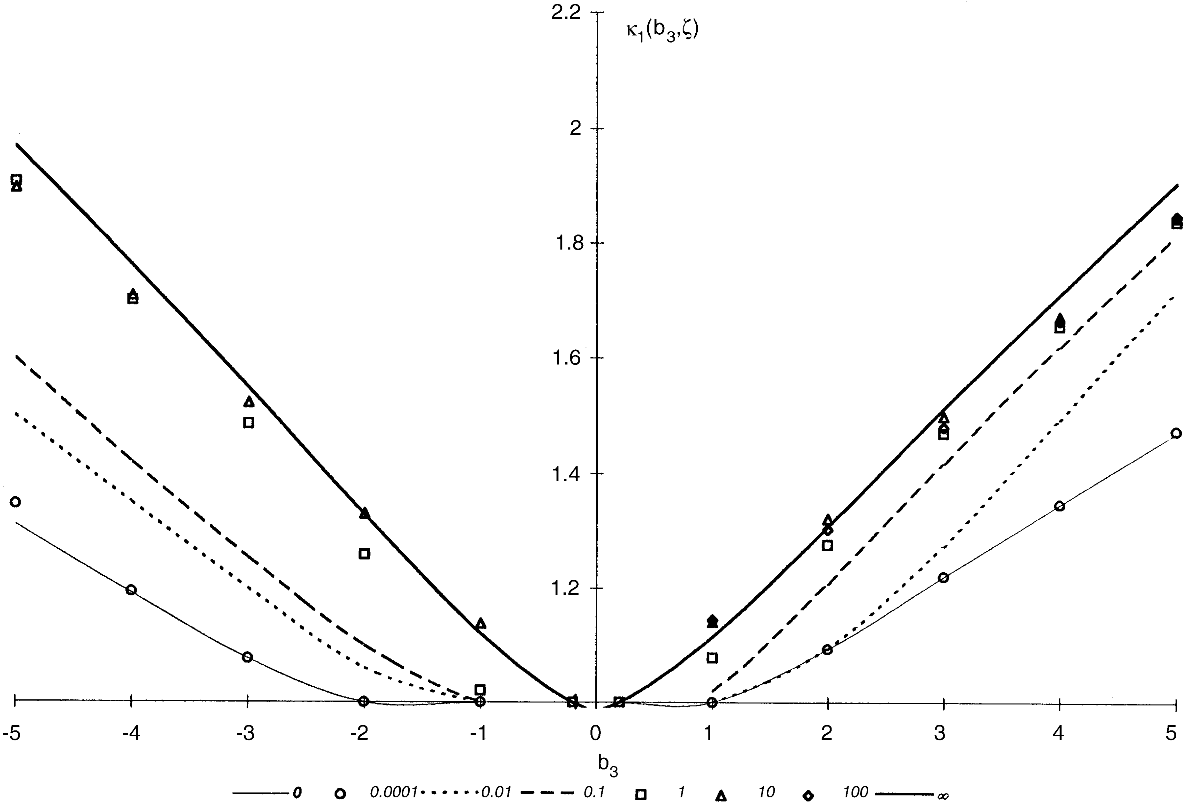

Fig. 4. TST dependence of κ_1 on b_3 at a few selected values for ζ, indicated on the plot.

Table 1
Value of a_i coefficients from Eq. (19) for the selected values of ζ

$k_1(b_3) = a_0 + a_1 b_3 + a_2(b_3)^2$		a_0	a_1	a_2
$\zeta = 1$	$b_3 < -1$[a]	0.7780	−0.2477	−0.0043
	$b_3 > 1$	0.8744	0.2063	−0.0027
$\zeta = 0.1$	$b_3 < -2$[a]	0.8405	−0.1145	0.0075
	$b_3 > 2$	0.7661	0.2279	−0.0037
$\zeta = 0.01$	$b_3 < -2$[a]	0.7905	−0.1295	0.0025
	$b_3 > 2$	0.7868	0.1297	0.0113

[a] For $|b_3| < 1$ or $|b_3| < 2$ equation describing κ_1 vs. b_3 has the form $k_1(b_3) = 1 + A_1 b_3 + A_2(b_3)^2$, where A_1 and A_2 can be found from the condition of function continuity at $|b_3| = 1$ or $|b_3| = 2$.

can fit the empirical formula:

$$\kappa_1(b_3) = a_0 + a_1 b_3 + a_2(b_3)^2, \quad |b_3| \le 5 \tag{19}$$

The numerical values for the a_i coefficients ($i = 0, 1, 2$) are listed in Table 1.

The curves shown in Fig. 4 indicate that κ_1 (b_3) is asymmetrical. Capture rate constants in the even case (q and Q have the same sign) are not the same as in the odd case (q and Q have opposite signs). This observations agrees with practically every other theoretical calculation [14,15,22–26]. The theory developed by Kosmas [27] is the sole exception yielding capture rate constant proportional to the square of qQ. Most of the calculated results indicate that capture rate constants in the odd case are larger than those in the even case. Only does average quadrupole orientation theory [23] suggest that the reverse happens. We have previously shown [15] that the first conclusion stems from the explicit or implicit assumption that $\zeta \to \infty$, while the second one from $\zeta \to 0$. Fig. 4 shows clearly the transition from one type of relationship to another as ζ decreases. Even though κ_1 decreases with decreasing ζ for both the even and odd case, the decrease is more pronounced for the latter case. The breakeven point corresponds to about $\zeta \cong 0.1$. There are few real ion/quadrupole systems for which ζ is of the order of 0.1. Therefore, the statement that capture rate constant in the odd case is always larger than that in the even case is not correct.

3. Comparison with experiment and other theroetical estimations

Maergoiz et al. [12] using the CT, method developed much more intricate empirical equation:

$$\kappa_1 = \left(\frac{1}{\pi^2\theta^2}\right)^{1/4} \kappa(\theta, M) \tag{20}$$

$$\ln[\kappa(\theta, M)] = a_0 + \left[\frac{a_1^2}{\sin h(z)} + \frac{z^2}{16}\right]^{1/2} \tag{21}$$

$$z = a_2 + \ln(\theta) \tag{22}$$

where a_0, a_1, a_2 are the empirical coeffcients while θ and M are analogs to b_3 and ζ in our notation.

$$\theta = (b_3)^{-4/3} \tag{23}$$

$$M = 0.5\zeta(b_3)^{8/3} \tag{24}$$

M is simply related to the Massey parameter that defines the level of nonadiabaticity in the system [12]. Other attempts [17,21,23–25,26–28] to describe the rate of ion/quadrupole capture were not general; either Hamiltonian was oversimplified or only some specific reactions were considered.

Table 2 assembles α and Q values for a few quadrupole molecules at most frequently studied temperatures. b_3 values at such temperatures are also included. It is seen that $|b_3|$ falls on very narrow range, $0 < |b_3| < 5$. Note that the upper limit corresponds to $T = 27$ K; at so low temperature the classical theories are of dubious value.

In Table 3 the values for κ_1 are reported for a few values of ζ and three not too large b_3. Estimates are based on our CT results and on the empirical formulae 20–22 derived by Maergoiz et al. [12] using different CT approach. Over the classical region of b_3, both CT versions differ by less than 2%. At the extremes of this region, ($|b_3| = 2$ and small ζ) the difference increases up to 6%. Apparently, the empirical formulae cease to be accurate. Since over the classical region the agreement between both versions of integration is so good, in further discussion, unless otherwise indicated, we will not make any differentiation between versions of CT.

Table 2
Value of b_3 parameter at a few selected temperatures for typical quadrupole molecules $\boldsymbol{M}$, most frequently studied in reaction with cations X^+

$\boldsymbol{M}$	a (Å^3)	$Q \times 10^{26}$ (esu cm^2)	b_3						Ref.
			$T = 300$ K	$T = 200$ K	$T = 100$ K	$T = 80$ K	$T = 67$ K	$T = 27$ K	
H_2	0.819	0.561	0.64	0.71	0.85	0.89	0.94	1.17	[24]
D_2	0.809	0.649	0.65	0.72	0.85	0.90	0.94	1.18	[24]
N_2	1.77	−1.4	−0.78	−0.86	−1.03	−1.08	−1.13	−1.42	[33]
O_2	1.6	−0.4	−0.24	−0.26	−0.31	−0.33	−0.35	−0.44	[24]
CO_2	2.65	−4.4	−1.80	−1.99	−2.37	−2.51	−2.62	−3.29	[33]
C_2H_2	3.33	7.2	2.48	2.75	3.27	3.46	3.61	4.54	[17]
C_6H_6	10.32	−5.6	−0.83	−0.92	−1.09	−1.15	−1.20	−1.51	[24]
C_6F_6	9.48	17.2	2.71	3.00	3.56	3.77	3.94	4.94	[26]
c-C_6H_{12}	10.87	13.2	1.88	2.08	2.47	2.61	2.73	3.42	[26]

Fig. 5 shows κ_1 (b_3) for two selected values of $\zeta \cdot \zeta = 10$ is on the border of the Su-Chesnavich plateau while $\zeta = 0.001$ is one time smaller than the lowest value observed for the realistic systems. It is seen that over the range $0 < |b_3| < 5$ our TST calculations give practically identical results, with only one exception, with those using the CT method. The deviations observed at $b_3 \geq 10$ are not meaningful since both theories do not account for the quantum effects that are likely to be of importance at so low temperature.

It is interesting that for b3 as negative as, say $b_3 \leq -10$, the discrepancies between TST and CT results nearly disappear. The reasons for the discrepancies for $b_3 \geq 10$, either loss of accuracy in numerical calculations or different assumptions, are not clear. Inspection of Fig. 5 reveals that the TST results are practically the same as the CT results. The sole exception already mentioned, the lack of good agreement between TST and CT, occurs at $\zeta = 10$ at $b_3 > 0$. The difference amounts to about 5% over the whole range of b_3 (3% when compared with our present CT results). The TST value is larger but this cannot be explained by the kinetic variational principle since the difference is not observed for other values of b_3 and ζ. We have no explanation for this discrepancy, which is unfortunate as it occurs at ζ corresponding to the majority of the real ion/quadrupole captures.

Still many ion/quadrupole processes undergo adiabatic capture as shown by Maergoiz et al. [12]. M is the measure of nonadiabaticity [21]. Table 4 lists M for frequently studied $C_6F_6 + X^+$ reactions [17,18,28,29] that feature very small values for ζ. Dynamics of adiabatic and nonadiabatic processes is expected to be significantly different leading to differences between κ_1 and κ_1^∞ at very large ζ [34]. The ratio defined in Eq. (25), and included in Table 4, can also serve as a measure of nonadiabaticity.

$$\Delta\% = \frac{\kappa_1^\infty - \kappa_1}{\kappa_1^\infty} \times 100 \tag{25}$$

Table 3
The values of κ_1 estimated by the CT method for a few selected ζ and three values for b_3 over the classical region of temperatures

$\log \zeta$	κ_1					
	$b_3 = -2$	$b_3 = -3$	$b_3 = -5$	$b_3 = 2$	$b_3 = 3$	$b_3 = 5$
−3	1.02 (1.06)	1.15 (1.13)	1.39 (1.37)	1.05 (1.12)	1.22 (1.22)	1.55 (1.49)
−2	1.08 (1.07)	1.20 (1.17)	1.63 (1.59	1.06 (1.12)	1.31 (1.25)	1.62 (1.63)
−1	1.17 (1.14)	1.37 (1.37)	1.81 (1.83)	1.16 (1.18)	1.38 (1.36)	1.73 (1.71)
0	1.27 (1.26)	1.48 (1.47)	1.93 (1.89)	1.24 (1.22)	1.41 (1.38)	1.76 (1.72)
1	1.29 (1.28)	1.48 (1.48)	1.93 (1.90)	1.24 (1.22)	– (1.38)	1.76 (1.72)

Values in brackets are taken from [12].

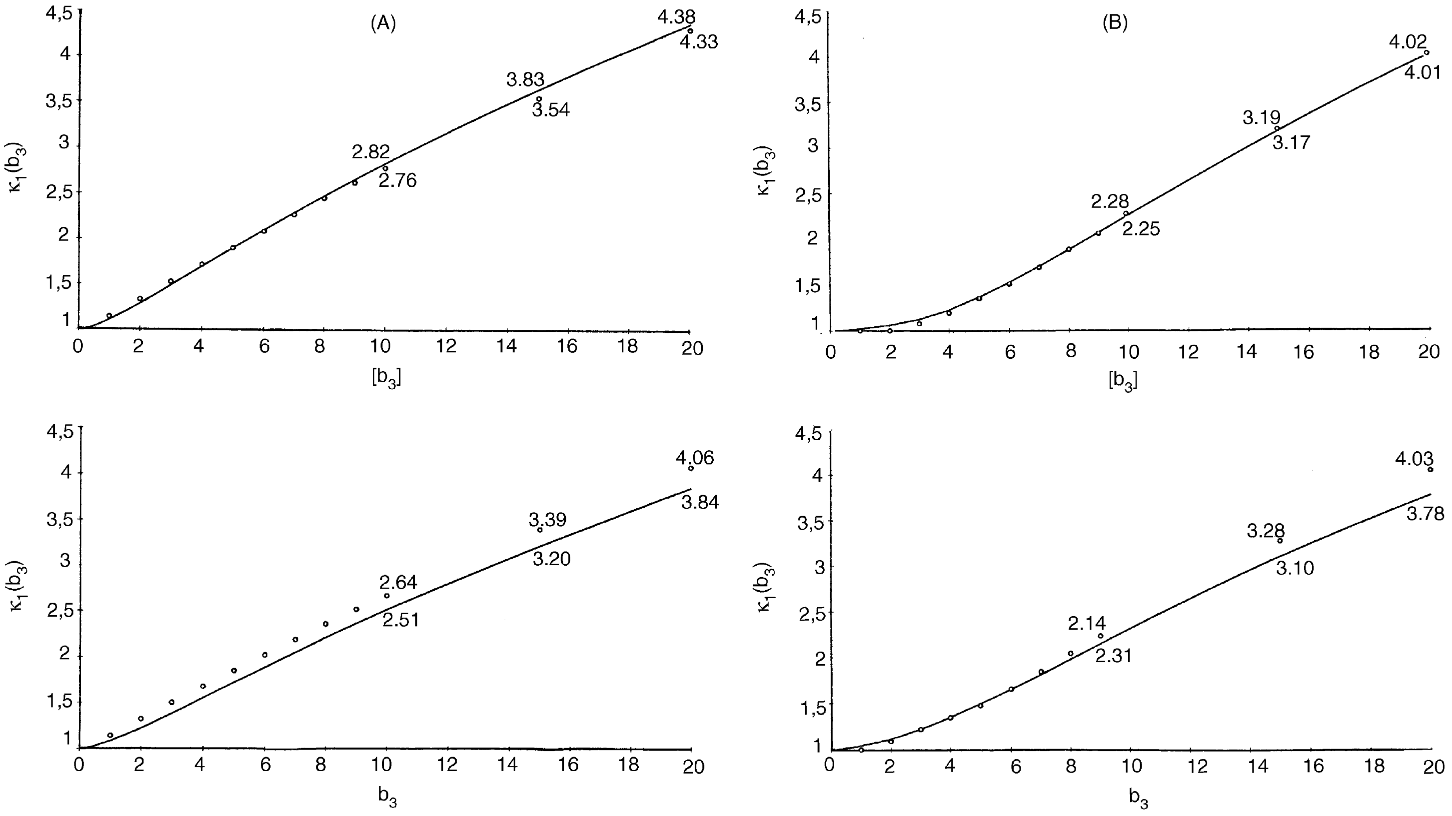

Fig. 5. Comparison between the TST obtained $\kappa_1(b_3)$ (this work—open circles) and $\kappa_1(b_3)$ obtained using the CT method [3] (solid lines). (A) $\zeta = 10$, (B) $\zeta = 0.001$. Top $b_3 < 0$, bottom $b_3 > 0$. κ_1 (b_3) estimated by both TST and CT for large values of $|b_3|$ ($|b_3| = 10$, 15 and 20) is shown at appropriate points of the plot.

Table 4
Contribution, $\Delta\%$, of the nonadiabatic motion of reactants to the TST capture rate constant for the reaction $C_6F_6+X^+$ in dependence on M (see Eq. (24))

X	T (K)	b_3	M	κ_1^{∞} [34]	κ_1	$\Delta\%$
He, $\zeta = 0.04$	600	2.28	0.18	1.36	1.19	12.5
	300	2.71	0.28	1.45	1.28	11.7
	67	3.94	0.77	1.69	1.53	9.5
	27	4.94	1.42	1.88	1.74	7.4
D_3, $\zeta = 0.06$	600	2.28	0.27	1.36	1.22	10.3
	300	2.71	0.42	1.45	1.30	10.3
	67	3.94	1.16	1.69	1.55	8.0
	27	4.94	2.13	1.88	1.80	4.0
N, $\zeta = 0.13$	600	2.28	0.59	1.36	1.29	5.0
	300	2.71	0.91	1.45	1.38	5.0
	67	3.94	2.50	1.69	1.62	4.0
	27	4.94	4.62	1.88	1.81	4.0

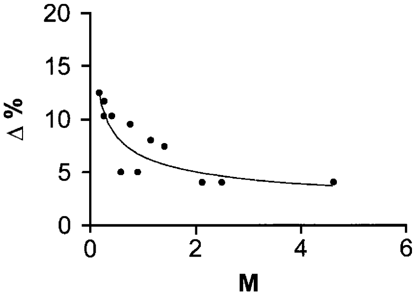

Fig. 6. Relative percentage contribution of the nonadiabatic effects to the TST capture rate constant on the dimensionless parameter M.

This ratio, as expected, depends on M. The form of such a relation is shown in Fig. 6. It can be seen that the larger the M the smaller the contribution of the nonadiabatic effects. Note that for the series of reactions involving, for instance, different ions, $\Delta(M)$ can only indicate the trend, not the precise function, as the points are considerably scattered around the line.

The nonequivocal $\Delta(M)$ can be obtained from a series of processes with $b_3 = \text{const}$; practically the problem is reduced to all of the reactions undergone by the same molecule at constant temperature. Note that according to Eq. (10), at constant b_3, $\Delta(M)$ is in fact a function of ζ. Thus, it is ζ that determines the contribution of nonadiabatic processes to the capture rate constant in the most precise fashion.

So far we have compared our results with those obtained by the classical trajectories method. As already mentioned other theoretical papers were not general but only concerned with some specific reactions. b_3 and ζ for the reaction of C_6F_6 with three different X^+ ions (X = He, C, N) at three different temperatures are listed in Table 5. Experimental data as well as the results of four theoretical calculations including one using TST are also included. Experimental

Table 5
Experimental rate constants for the reaction of C_6F_6 with selected cations X^+ at three different temperatures, and theoretical values for the capture rate constants for these reactions estimated with use of three different methods

X	ζ	T (K)	b_3	κ_{exp}	κ_1[a]	κ_1[b]	κ_1[c]	κ_1[d]	κ_1[e]
He	0.04	297	2.71	1.13	1.31	1.21	1.34	1.28	1.27
		67	3.94	0.96	1.53	1.39	1.55	1.53	1.51
		27	4.94	0.83	1.71	1.64	1.71	1.74	1.76
C	0.11	297	2.71	1.21	1.30	1.25	1.34	1.37	1.32
		67	3.94	1.12	1.52	1.63	1.55	1.62	1.57
		27	4.94	1.17	1.71	1.86	1.71	1.81	1.75
N	0.13	297	2.71	1.21	1.31	1.33	1.34	1.38	1.33
		67	3.94	1.11	1.53	1.61	1.55	1.62	1.57
		27	4.94	1.01	1.71	1.64	1.71	1.81	1.75

[a] Bhowmik and Su CT calculations from paper [24].

[b] Mendas and Milutinovic CT calculations from paper [26].

[c] Bates and Mendas calculations from paper [22].

[d] Present TST calculations.

[e] Present CT calculations.

Table 6
Comparison between experimental and theoretical capture rate constants for the reaction $CO_2 + X^+$

X	ζ	κ_{exp} [a]	κ_1	κ_1^{eff}
OH	1.22	1.24	1.23	1.27
H	0.10	1.01	1.08	1.10
H_2	0.19	0.86	1.09	1.10
H_3	0.28	1.10	1.10	1.12
F	2.57	1.20	1.25	1.31
N_2H	1.74	1.18	1.23	1.27
HCO	1.66	1.02	1.23	1.28
CO	1.70	1.20	1.23	1.28
CH	1.00	1.33	1.21	1.26
CH_2	1.05	1.37	1.21	1.26
CH_4	1.27	0.94	1.20	1.27
CN	1.97	1.29	1.25	1.31
CCN	2.02	1.31	1.25	1.31
ArH	4.12	1.10	1.29	1.32

$T = 300\,K$, $b_3 = -1.80$, $b_3^{eff} = -2.03$.

[a] Experimental data from [19,20].

capture rate constants are always smaller than those obtained by theoretical estimations. The difference is small at 297 K but at 67 K and especially at 27 K it amounts up to 60% which may indicate the occurrence of quantum effects. As shown by Maergoiz et al. [12]. at very low temperatures quantum effects reduce κ_1 down to unity. The difference between our estimates and those obtained using other theoretical methods are slight, mostly about 2–3%. The largest difference at 27 K amounts to about 6%. All of the processes listed in Table 5 involve $b_3 > 0$. For the sake of comparison our TST estimates for the reactions $CO_2 + X^+$ and $N_2 + X^+$ that feature $b_3 < 0$ are compared with experiment in Tables 6 and 7. The temperatures were usually high, 300 K, only in some N_2 reactions 80 K–at such temperatures quantum effects are unlikely to be important. The agreement with experiment is satisfactory. It can be even improved, as is indicated by the data in pertinent columns of Tables 6 and 7, by taking into account the polarizability anisotropy [13].

4. Conclusions

Capture rate constant for the ion/linear quadrupole was estimated using the microcanonical version of the transition state theory and CT method. The total energy and the resultant total angular momentum were rigorously conserved. Two dimensionless parameters, ζ and b_3, affect the result. ζ describes contributions of the orbital and rotational momenta to the resultant momentum. At very small values of ζ the partial capture rate constant is defined for the resultant angular momentum over the range $0 \leq J \leq (2IE)^{1/2}$.This range widens as ζ increases. The B_3 (or b_3) parameter describes the energy/temperature dependence of κ_1. At fixed b_3 all of the $\kappa_1(\zeta)$ functions exhibit a characteristic behaviour: the region of ζ independence (the first plateau) at very small ζ followed by the transitional region (κ_1 increasing with increasing ζ, hence, with increasing reduced mass of the system) and the second plateau, called by us as the Su-Chesnavich plateau [10]. The transitional region covers many of the realistic ion/quadrupole systems. b_3 can be either positive (the even case) or negative (the odd case). On both the plateaus the relations with respect to the sign on b_3 are opposite. At $\zeta \rightarrow 0$ the capture rate constant is larger for the even case; at $\zeta \rightarrow \infty$ the trend is reversed. The breakeven point occurs at about $\zeta \cong 0.1$. A majority of the realistic ion/quadrupole systems feature larger

Table 7
Comparison between experimental and theoretical capture rate constants for the reaction $N_2 + X^+$

X	ζ	T (K)	b_3	b_3^{eff}	κ_{exp}	κ_1	κ_1^{eff}
ArH_3	73.8	300	−0.78	−0.88	1.17 [30]	1.08	1.10
ArH_3	73.4	80	−1.08	−1.77	1.27 [31]	1.15	1.15
ArH	72.4	300	−0.78	−0.88	1.05 [19]	1.08	1.10
H_2	8.1	300	−0.78	−0.88	1.19 [32]	1.08	1.10
H_3	11.8	80	−1.08	−1.17	1.00 [31]	1.15	1.13
F	49.2	300	−0.78	−0.88	1.20 [19]	1.08	1.10

values for ζ but some cover precisely this transitional region, and the sign dependence has to be considered for every specific case.

The results of the TST dependence of κ_1 on the energetic and molecular dimensionless parameters b_3 and ζ are in excellent agreement with those obtained using the CT methods. Only at extremely low temperatures, corresponding to $|b_3| \geq 10$, does the agreement deteriorate. Probably both the methods are inadequate at very low temperatures. M is a useful measure of nonadiabaticity of the system dynamics only at $b_3 = \text{const}$. It looks as though ζ should be preferred as a nonequivocal measure of the nonadiabaticity of motion. TST estimates are in good agreement with other theoretical calculations as well as with experiment provided that the temperature is not too low.

References

[1] E.E. Nikitin, Theory of Elementary Atomic and Molecular Processes in Gases, Khimia, Moscow, 1970, p. 50.
[2] J. Turulski, J. Niedzielski, J. Phys. Chem. 88 (1984) 2745.
[3] W.J. Chesnavich, T. Su, M.T. Bowers, in: P. Ausloos (Ed.), Kinetics of Ion–Molecule Reactions, Plenum Press, New York, 1979, p. 35.
[4] W.J. Chesnavich, T. Su, M.T. Bowers, J. Chem. Phys. 72 (1980) 2641.
[5] W.J. Chesnavich, M.T. Bowers, Prog. React. Kinet. 11 (1982) 137.
[6] J. Troe, Chem. Phys. Lett. 122 (1985) 425.
[7] J. Troe, J. Chem. Phys. 87 (1987) 2773.
[8] D.R. Bates, Proc. R. Soc. A 384 (1982) 289.
[9] K. Sakimoto, Chem. Phys. 85 (1984) 273.
[10] J. Turulski, J. Niedzielski, Mol. Phys. 67 (1989) 181.
[11] A.I. Maergoiz, E.E. Nikitin, J. Troe, V.G. Ushakov, J. Chem. Phys. 105 (1996) 6263.
[12] A.I. Maergoiz, E.E. Nikitin, J. Troe, V.G. Ushakov, J. Chem. Phys. 105 (1996) 6270.
[13] B. Pezler, J. Turulski, J. Niedzielski, J. Chem. Soc., Faraday Trans. 89 (1993) 655.
[14] T. Su, W.J. Chesnavich, J. Chem. Phys. 76 (1982) 5183.
[15] J. Turulski, Chem. Phys. 143 (1990) 185.
[16] J. Turulski, J. Niedzielski, in: W. Hase (Ed.), Advances in Classical Trajectory Methods, Vol. 2, JAI Press, 1994, p. 223.
[17] P.K. Bhowmik, T. Su, J. Chem. Phys. 84 (1986) 1432.
[18] C. Rebrion, J.B. Marquette, B.R. Rowe, N.G. Adams, D. Smith, Chem. Phys. Lett. 136 (1987) 495.
[19] V.G. Annicich, Ap. J. Suppl. Series 84 (1993) 215.
[20] V.G. Annicich, J. Phys. Chem. 6 (1994) 1469.
[21] I. Mendas, P. Milutinovic, Chem. Phys. 153 (1991) 73.
[22] D.R. Bates, I. Mendas, Proc. R. Soc. A 402 (1985) 245.
[23] T. Su, M.T. Bowers, Int. J. Mass Spectrom. Ion Phys. 17 (1975) 309.
[24] P.K. Bhowmik, T. Su, J. Chem. Phys. 94 (1991) 6444.
[25] S.C. Smith, J. Troe, J. Chem. Phys. 97 (1992) 5451.
[26] I. Mendas, P. Milutinovic, Chem. Phys. 134 (1989) 47.
[27] A.M. Kosmas, J. Phys. Lett. (Paris) 46 (1985) L799.
[28] F. Celli, G. Weddle, D.P. Ridge, J. Chem. Phys. 73 (1980) 801.
[29] B.R. Rowe, in: T.J. Millar, D.A. Williams (Eds.), Rate Coefficients in Astrochemistry, Kluwer Academic Publishers, Dordrecht, 1988, pp. 135–152.
[30] C. Praxmarer, A. Hansel, W. Lindinger, J. Chem. Phys. 100 (1994) 8884.
[31] D. Smith, P. Spanel, D.K. Bedford, Chem. Phys. Lett. 191 (1992) 587.
[32] J. Glosik, Int. J. Mass Spectrom. Ion Phys. 139 (1994) 15.
[33] J. Liu, T. Su, J. Chem. Phys. 95 (1991) 6471.
[34] J. Turulski, B. Pezler, J Niedzielski, Chem. Phys. 166 (1992) 115.